Basic Analysis on Building Damages by Tsunami due to The 2011 Great East Japan Earthquake Disaster Using GIS

Kunihiro Amakuni
Pacific Consultants Co. Ltd., Tokyo, Japan

Naoto Terazono, Toshio Yamamoto& Takahisa Enomoto
Kanagawa University, Yokohama, Kanagawa, Japan

SUMMARY:
In Japan, destructive damage occurred by the offing massive earthquake of the Tohoku district. The Earthquake with Mw9.0 has occurred in 11th March, 2011. Major damages, such as about 20,000 dead or missing people and about 250,000 collapsed buildings, were caused by big tsunami, whose height has been recorded more than 10m high. Main damaged areas are located along the Pacific coast of three prefectures, Iwate, Miyagi and Fukushima Prefectures. We were focusing to the damages of wooden buildings caused by tsunami in Miyagi Prefecture. In this paper, we would like to present the summary of this basic research on the relationship between building damages and tsunami element which is consisting of wave speed, wave height and wave force. The element was estimated by tsunami simulation results. We hope that these results are useful for the future tsunami disaster prevention.

Keywords: The 2011 Great East Japan Earthquake Disaster, Tsunami, Building Damages

1. INTRODUCTION

At 14:46 PM on March 11, 2011, a magnitude 9.0 earthquake has occurred at the offing Pacific coast between the Tohoku and Kanto regions. The name of this earthquake is the 2011 Off Pacific Ocean Coast in Tohoku District Earthquake (hereinafter referred to as “the offing massive earthquake of the Tohoku district”). Major damages, such as about 20,000 dead or missing people and about 250,000 collapsed buildings, were caused by big tsunami, whose height has been recorded more than 10m high. Main damaged areas are located along the Pacific coast of three prefectures, Iwate, Miyagi and Fukushima Prefectures. In Iwate Prefecture, the north part of damaged area, the coast area is geographically formed by Ria Coast and tsunami was influenced by this geographical sea coast shape. Consequently tsunami height was higher than 15m to 20m. Oppositely, in Miyagi Prefecture and Fukushima Prefecture, the middle and south part of damaged area, the Pacific coast is geographically normally flat shape, such as called as Coast Plain. And Tsunami of higher than 10m has affected seriously and has reached up to 4 - 5km of inland from coast line. This area is constituted by newly developed residential part and rural part in which farmer's houses and agricultural fields are located. We have obtained the detailed building information organized by Miyagi prefectural office and have obtained, also, the calculated tsunami height data and flowing vector data simulated by the Tohoku University, Graduate School of Engineering, Disaster Control Research Center. And we could use the GIS oriented database presented by ESRI. And also we could use the detailed map of tsunami affected area and the aero photographs of damaged area before and after the earthquake distributed from GSI, Geospatial Information Authority of Japan, using the internet website. Based on these data, we have investigated the building damage caused by tsunami using graphical analysis function already installed in Arc-GIS. Then we were focusing to the damages of wooden buildings in Miyagi Prefecture and we piled up the maps of building shape combined attribute of building structure, and tsunami affected area in order to identify the damaged zone due to tsunami and also piled up the result of simulated tsunami height and flowing vectors in order to estimate tsunami wave force. And also we compared the aero photographs before and after the earthquake in order to identify the damages caused by tsunami.

Through these analyses, we have summarized the influence of tsunami element on buildings damages. In this paper, we would like to present the summary of this basic investigation on the relationship between building damages and tsunami element which is consisting of wave speed, wave height and wave force. The element was estimated by tsunami simulation results. We hope that these results are useful for the future tsunami disaster prevention.

2. OUTLINE OF EARTHQUAKE AND TSUNAMI

The 2011 off the Pacific Coast of Tohoku Earthquake, Mw9.0, generated large tsunami in the Tohoku and Kanto regions of the northern part of Japan (EERI, 2011). This was a thrust earthquake occurring at the boundary between the North American and Pacific plates. A Mw 7.5 foreshock preceded the mainshock on March 9 and many large aftershocks including two Mw 7 class aftershocks followed the mainshock. This subduction earthquake generated a tsunami of unprecedented height and spatial extent along the coast of the main island of Honshu. Japan is located near the meeting point of the Eurasian Plate, the Philippines Sea Plate, the North American Plate, and the Pacific Plate (see **Figure 1**). Off the Tohoku coast, the Japan Trench forms where the Pacific Plate subducts beneath the North American Plate. The earthquake epicenter was about 100 km offshore, causing ground shaking to VI^{+} - VII in Japan Meteorological Agency (JMA) Intensity Scale or less in most of Honshu Island. The earthquake successively ruptured over an area of approximately 500 km by 200 km. At the mega-thrust fault, vertical movement of the ocean floor is estimated by JMA to be at least 3 m upward and 24 m laterally.

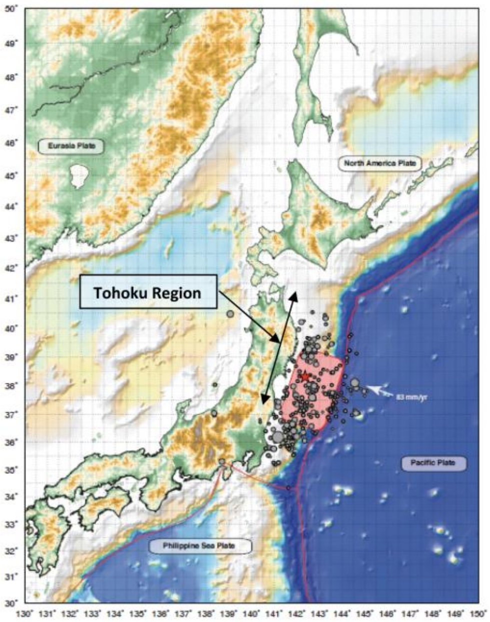

Figure 1 Tectonic setting of Japan with epicenters of the great East Japan earthquake and its aftershocks off the Tohoku region of Honshu Island (source: USGS).

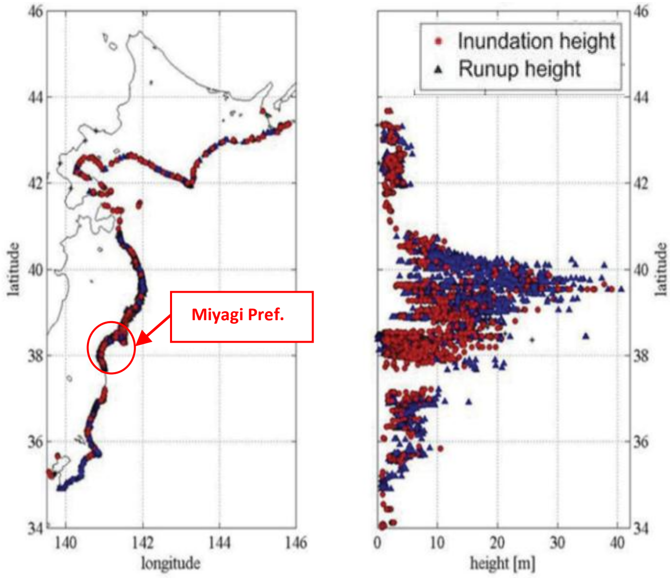

Figure 2 Inundation and runup heights reported by the Tohoku Earthquake Tsunami Joint Survey Group.

JMA reported the tsunami heights observed at coastal tide gauges. According to JMA, the tsunami heights were less than 3 m along the coasts of Hokkaido to Aomori prefectures, and more than 4 m along the coasts of the Tohoku region stopped recording after the first tsunami arrival, because of power failure of the stations were damaged by the tsunami. Later JMA retrieved the tide gauge records on site and announced that the observed tsunami heights were more than 8.5 m at Miyako, more than 8.0 m at Ofunato, more than 7.6 m at Ayukawa, and more than 9.3 m at Soma. Tsunami heights in the coastral areas of Japan were measured and reported by the 2011 Tohoku Earthquake Tsunami Joint

Survey Group. The field surveys were mainly conducted along the Pacific coasts from Hokkaido to Okinawa. The survey results all end up on the internet site and are being updated appropriately (see **Figure2**). According to the preliminary survey results, inundation or runup heights were about 5 m in the Pacific coasts of Hokkaido, up to 10 m in Aomori and Chiba prefectures, more than 30 m in some locations along the Sanriku coasts of Iwate, up to 20 m in Miyagi prefecture (NILIM & BRI, 2011).

3. RESEARCH AREA IN MIYAGI PREFECTURE

As a result of the offing massive earthquake of the Tohoku district, strong shaking was observed in eastern Japan and a violent tsunami struck the Pacific coast of Miyagi, Iwate, and Fukushima prefectures. The author of this paper investigated part of the coast in Iwate and Miyagi prefectures on April 8 to 10, 2011. It was considered that, the damages caused by seismic motion could be seen only at broken roof tiles of a few houses. And the completely collapsed buildings and overwhelming number of deaths were considered to be due to the tsunami. The state of tsunami damage varied greatly with just a small difference in elevation, and even in areas where most buildings were demolished, buildings considered to be only lightly damaged were found (see **Photograph 1**).

Photograph 1.Damaged wooden buildings due to tsunami

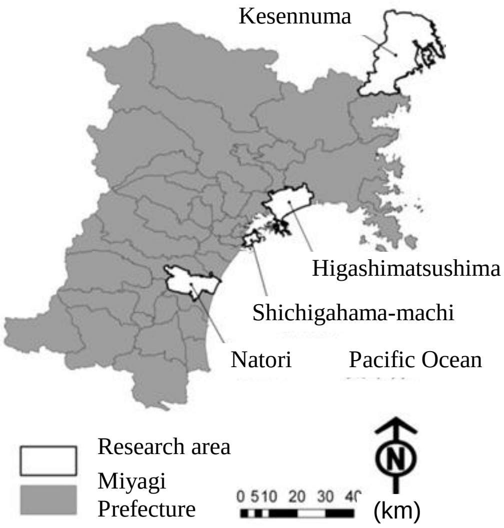

Figure 2 Location of research areas

The collection and analysis of wide-area information on earthquake disasters is extremely important in considering future disaster prevention and mitigation measures. In this research, information was collected in four towns and cities on Miyagi Prefecture's coast (Natori, Shichigahama-machi Higashimatsushima, and Kesennuma) (see **Figure 2**) using the spatial analysis function of Esri's ArcGIS. This paper presents the results of this research. This paper organizes/analyzes the information on damage caused by the offing massive earthquake of the Tohoku district, and attempts to construct vulnerability functions by integrating assessment of damage to housing using aerial photographs and tsunami inundation analysis results.

4. PREPARATION OF BUILDING DATA

Geocoding is carried out using a free GIS service via Google based on addresses in the database (2010 version) of buildings in Miyagi Prefecture. From the obtained coordinate values, point data with attribute values of year built/type of structure is prepared using ArcGIS. Spatial join of the prepared point data that coincides with ordinary house frame polygons is done using Esri/Zenrin, and data obtained from the spatial join is taken as building data (See **Figure 3**). Addresses are indicated using the residential address (jyukyo hyoji, Japanese) or the lot number (chiban hyouji, Japanese), and this indication differs according to district and district boundary. In order to obtain coordinate values, residential address indication (jyukyo hyoji, Japanese) is required and there are some areas in which the distribution of building data is not balanced.

Using the results of reproduction calculations of the tsunami inundation flow resulting from this earthquake carried out by the Tohoku University, Graduate School of Engineering, Disaster Control Research Center, values for inundation flow are spatially joined to building data. Of flow velocities V_X, V_Y, V (composite value of absolute values in X, Y directions) and inundation depth D, V and D are used. Because the reproduction calculation results are raster data, they are converted to point data (See **Figure 4**).

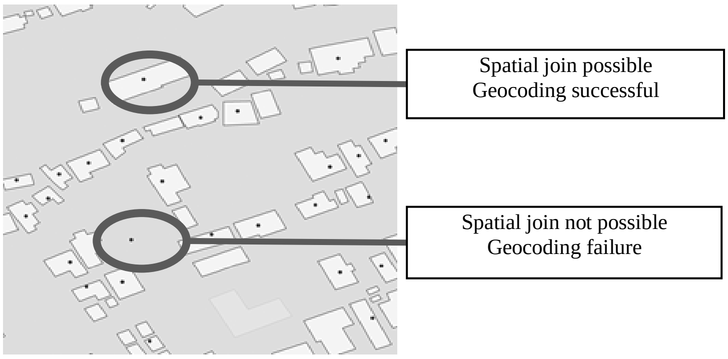

Figure 3 Preparation of building data

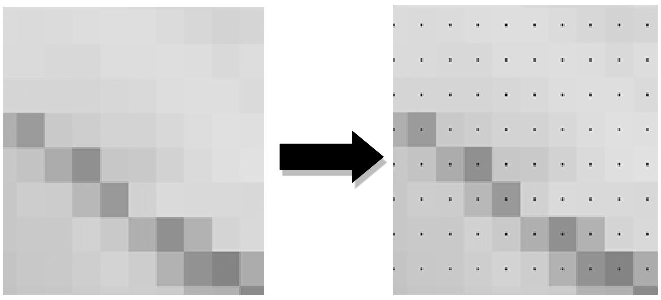

Figure 4 Conversion of raster cell values to point data

The attribute values of the point data obtained are linked to the building data. The energy exerted as external force by the tsunami on a building (tsunami external force, F) is calculated from flow velocity in the reproduction calculation results using Equation (1). A value of 1.03 (10^3 kg/m^3) taken from the Chronological Scientific Tables (Rika Nenpyo, Japanese) is used for ρ (density of seawater). When providing attribute values using spatial join, the search radius is taken as 3 m. The results shown in **Table 1** are obtained accordingly.

$$F = \frac{1}{2}\rho V^2 (N/m^2) \qquad (1)$$

Table 1 Estimated Numbers of houses and buildings

Descriptions	Natori	Shichigahama	Higashi Matushima	Ksennuma	Total
ordinary house (frame polygons)	28,156	9,858	23,131	35,421	96,566
Buildings (obtained from the spatial join)	10,294	4,243	10,311	13,763	39,241
Buildings Inundated (estimated)	868	820	3,423	3,542	8,653
wooden	744	766	3,182	3,230	7,921
Non-wooden	124	54	242	312	732

5. ASSESSMENT OF BUILDING DAMAGE USING AERIAL PHOTOGRAPHS

When assessing the extent of damage to buildings (Horie et al. 2003), the “Aerial Photographs of the Area Affected by the Great East Japan Earthquake" published by the Geospatial Information Authority of Japan are used to visually compare photographs taken directly after the earthquake and photographs taken 2~6 months after the earthquake (GIA 2011). Building assessment is carried out in ArcMap (Kawasaki et al. 2008) and damage assessment attribute values are provided for the building data. Based on the assessment method, assessment patterns were classified into 3 categories, that are 1) Light or no damage, 2) Heavy or medium damage, 3) Washed away or collapsed. (See **Table 2**). The results of the damage assessment are shown in **Table 3**. Flow velocity and distribution of buildings according to damage in Natori are shown in **Figure 5** as an example.

Table 2 Damage assessment method using aerial photographs

	Immediate aftermath of Disaster	After 2 to 6 months	
1	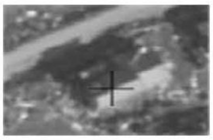	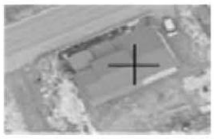	Building Shape maintained
2	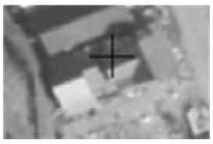	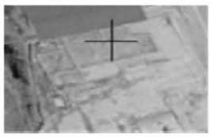	Removal of buildings and rubble after 2 to 6 months
3			Immediate aftermath of disaster, buildings collapsed or washed away

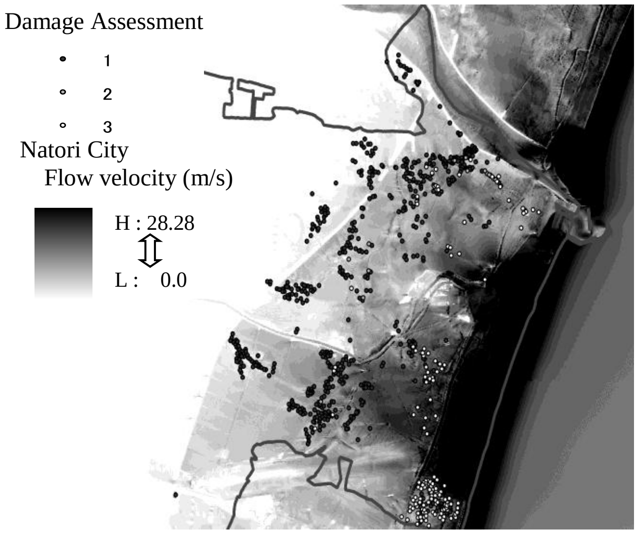

Figure 5 Flow velocity and distribution of buildings according to damage in Natori

Table 3 Damage assessment results by region

Descriptions	Natori	Shichigahama	Higashi Matushima	Ksennuma	Total
Assessment pattern 1	671	420	2,590	1,591	5,272
Assessment pattern 2	13	23	1	2	39
Assessment pattern 3	184	377	832	1,949	3,342

6. PREPARATION OF VULNERABILITY FUNCTIONS

Vulnerability functions are prepared for building data for which attribute values are provided according to building assessment based on aerial photographs. Vulnerability functions are also called fragility functions, and vulnerability functions that quantitatively represent the extent of building damage caused by seismic motion describe collective resistance of a group of buildings against strength of ground shaking and are used to evaluate the extent of damage to groups of buildings in a certain area. Research on vulnerability functions using extensive damage data from the Southern Hyogo Prefecture Earthquake has been reported by several groups, but the Murao & Yamazaki's method (Murao et al. 2000) has become the favoured method. Examples of vulnerability functions related to tsunami include those constructed for Okushiri Island by Koshimura & Kayaba as a result of the 1993 Hokkaido Nansei-Oki Earthquake tsunami (Koshimura 2010).

First, in order to equalize the weighting of building data for each class, building data is sorted into ascending order of hydrodynamic size of tsunami and grouped into a certain number of samples. In this research, damage ratios were found by dividing the data into 10 classes. The index value representing each class is expressed using the average value, and damage ratios are calculated by dividing the damaged buildings belonging to the class by the total number of buildings. As an example, basic numbers for flow velocity over the entire subject area are shown in **Table 4** and damage ratios found from these flow velocities are shown in **Figure 6**.

Table 4 Class and basic numbers (Example: Flow velocities for entire subject area)

Building Total	Ave. Vel.	Vel. Max.	Vel. Min.	Assessment pattern 1	Assessment pattern 2	Assessment pattern 3	Complete-collapsed rate
792	0.167	0.33	0.01	786	1	5	0.006
792	0.473	0.63	0.33	768	1	23	0.029
792	0.837	1.00	0.63	732	4	56	0.071
792	1.433	1.76	1.10	647	1	144	0.182
792	2.070	2.41	1.76	485	7	300	0.379
792	2.747	3.05	2.41	422	8	362	0.457
792	3.402	3.78	3.05	351	5	436	0.551
792	4.217	4.74	3.78	321	6	465	0.587
792	5.259	5.83	4.74	156	5	631	0.797
792	7.001	12.00	5.83	111	0	681	0.859

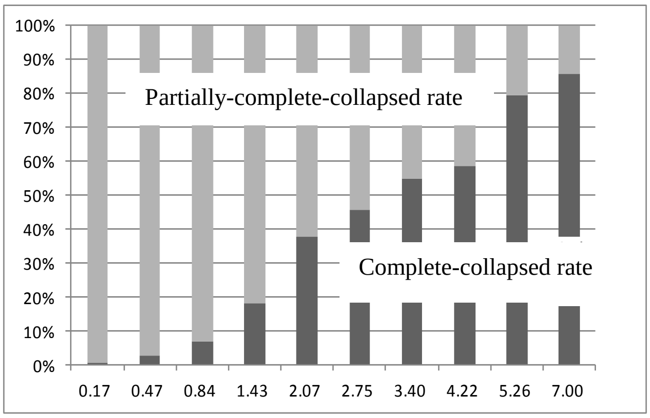

Figure 6 Class values and collapse rates for wooden buildings over entire subject area (flow velocity [m/s])

In this research, following the Murao & Yamazaki's method, vulnerability functions are constructed using Equation (2), assuming that the probability PR of a damage ratio R or above arising in response to a certain external force (x) can be represented by a lognormal distribution using the cumulative distribution function of the standard normal distribution Φ(x).

$$P_R = \phi\{\ln(x)\} - \lambda/\zeta \qquad (2)$$

Here, λ and ζ are the mean value and standard deviation of ln(x).

First, using the NORMSINV function, the damage ratios and the coordinate value Z_i of the corresponding normal distribution are found. A scatter diagram is drawn by plotting data ln(x) (horizontal axis) and coordinate value Z_i (vertical axis) on probability paper, and a regression line is drawn on the graph using the least-squares method. If the points are scattered near this straight line, the data is considered to have a normal distribution (see **Figure 7**). R^2, mentioned hereafter, is called the coefficient of determination, and it represents the proportion of variability in the entire data set that can be explained by the regression equation. Also, if the gradient of the regression line is taken as "a" and the intercept as "–b", then λ=b/a and ζ=1/a. In this way, parameters λ and ζ, which are required for preparing vulnerability functions, are found.

As an example of a vulnerability function obtained from regression using the lognormal distribution function of Equation (2), the vulnerability function for wooden buildings in the entire subject area is shown in **Figure 8**.

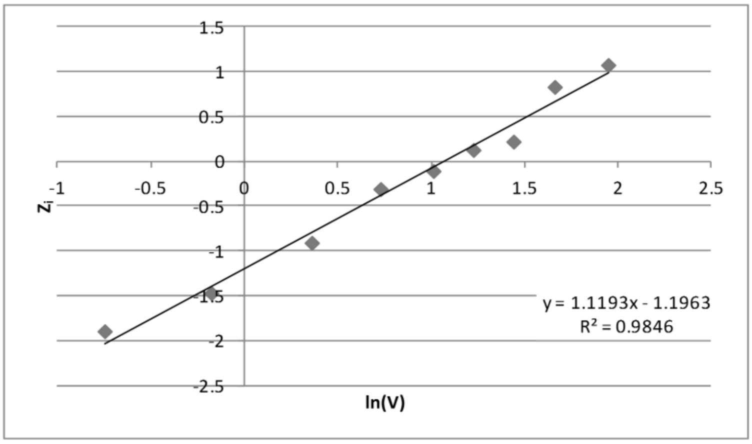

Figure 7 Probability paper plot and regression line of damage ratios

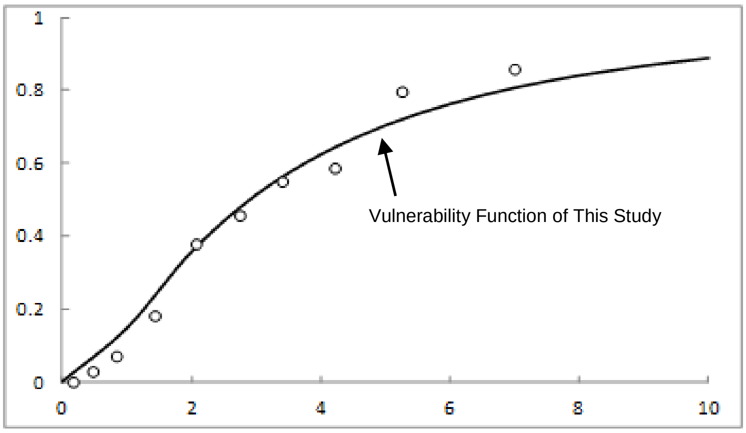

Figure 8 Vulnerability function for wooden buildings in entire subject area (tsunami flow velocity) [m/s]

7. RESULTS OF VULNERABILITY FUNCTION

The vulnerability functions and respective graph parameters for wooden buildings in regard to tsunami inundation flows for each town and construction period obtained through the above-mentioned method are shown (See **Figures 9 and 10**). Construction periods are divided into 3 groups: 1963 and earlier, 1964~1981, and 1982 and later. The damage ratios for wooden buildings according to period are shown in **Figure 10(d)**.

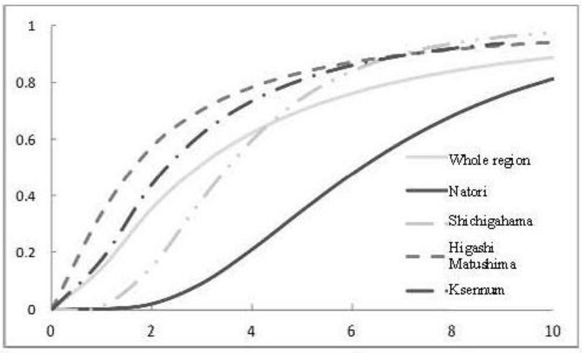

Region	R^2	λ	ζ
Whole region	0.972	1.070	1.010
Natori	0.895	1.820	0.541
Shichigahama	0.960	1.250	0.541
Higashi Matushima	0.964	0.598	1.150
Ksennuma	0.937	0.824	0.890

(a) Damage ratio and Tsunami flow velocity [m/s]

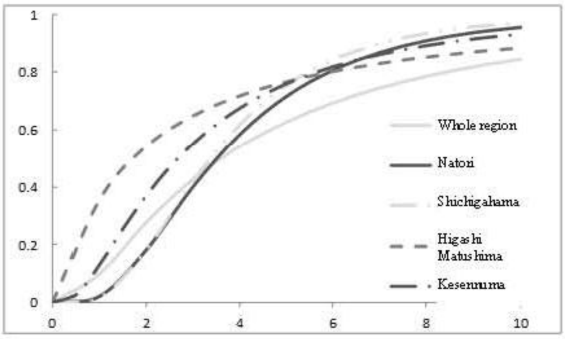

Region	R^2	λ	ζ
Region whole region	0.899	1.280	1.010
Natori	0.931	1.240	0.446
Shichigahama	0.766	1.210	0.577
Higashi Matushima	0.786	0.529	1.480
Ksennuma	0.927	0.981	0.888

(b) Damage ratio and Inundation depth [m]

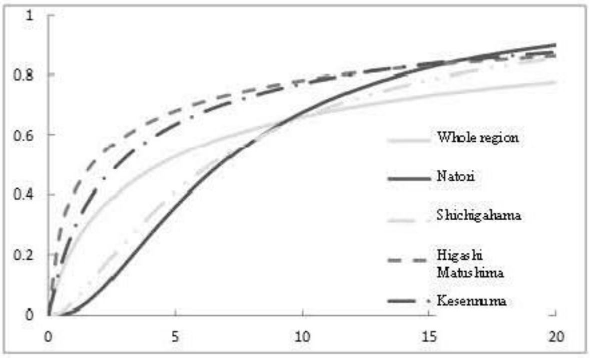

Region	R^2	λ	ζ
Region whole region	0.978	1.480	1.970
Natori	0.896	1.810	0.540
Shichigahama	0.959	1.860	1.080
Higashi Matushima	0.967	0.556	2.230
Ksennuma	0.944	1.010	1.740

(c) Damage ratio and Tsunami external force [KN/m^2]

Figure 9 Summary of vulnerability functions for wooden buildings

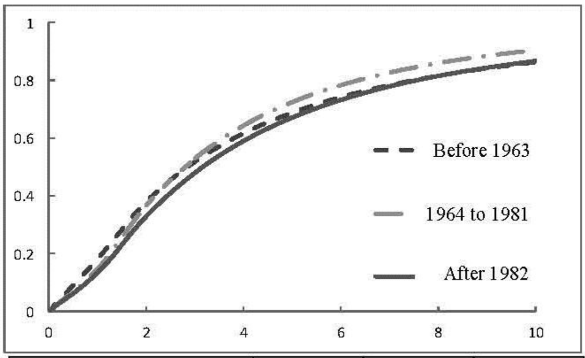

Construction year	R^2	λ	ζ
before 1963	0.881	1.05	1.15
1964 to 1981	0.882	1.03	0.98
After 1982	0.876	1.15	1.04

(a) Damage ratio and Inundation depth [m]

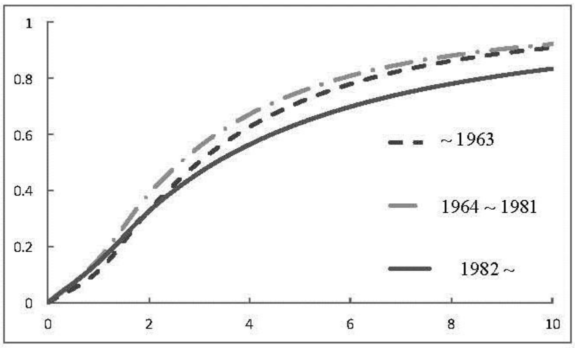

Construction year	R^2	λ	ζ
before 1963	0.917	1.51	1.66
1964 to 1981	0.939	1.36	1.67
After 1982	0.990	1.75	2.23

(b) Damage Ratio and Tsunami Flow velocity [m/s]

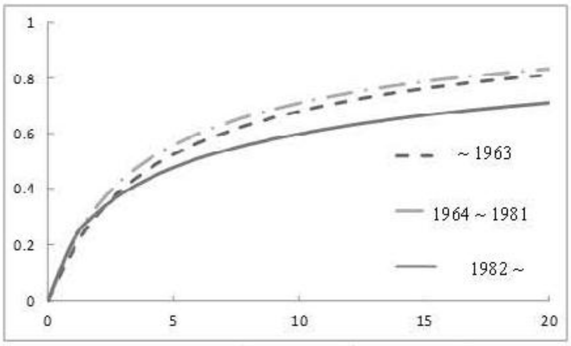

Construction year	R^2	λ	ζ
before 1963	0.897	1.10	0.90
1964 to 1981	0.936	0.97	0.95
After 1982	0.981	1.20	1.13

(c) Damage ratio and Tsunami external force [KN/m^2]

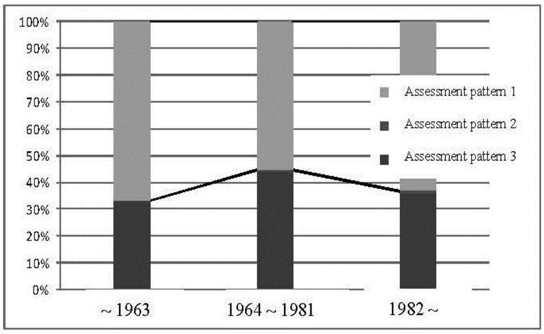

Descriptions	Before 1963	1964 to 1981	After 1982	Total
Assessment pattern 1	1,105	1,910	1,765	4,780
Assessment pattern 2	4	16	18	38
Assessment pattern 3	547	1,535	1,021	3,103

(d) No. of wooden buildings damaged and damage ratio for construction year

Figure 10 Vulnerability functions and damage ratios for wooden buildings according to period

8. DISCUSSION AND CONCLUSION

(a) Overall, the coefficients of determination for inundation water depth are lower than those for flow velocity and tsunami external force, and correlation between inundation water depth and collapse rate is considered to be low. In regard to tsunami external force, the coefficients of determination are all above 9.0, and a high correlation is seen. Also, there is quite a difference in collapse rate of wooden buildings according to area. In Shichigahama-machi and Kesennuma, where the topography of the coast is complicated, it can be seen that the collapse rate increases in an earlier class than in the other two areas. And, from a tsunami flow velocity of approximately 4 m/s and above, a fairly gentle gradient is shown. In contrast, in Higashimatsushima and Natori, the vulnerability functions show a fairly gentle gradient up to a tsunami flow velocity of approximately 2~3 m/s, and from there also the graph shows a gradual rise.

(b) A slight difference can be seen in the collapse rate of wooden buildings according to construction year. Buildings constructed before the 1981 revision of the Earthquake Resistant Standards have, overall, a higher collapse rate than buildings constructed later. The coefficients of determination for inundation water depth are inferior to the others in this case as well.

(c) From the above it is evident that topography and building location have a greater influence on building damage caused by a tsunami than construction year.

ACKNOWLEDGEMENTS

The authors are grateful to have the permission to use the result of Tsunami Simulation performed by the Tohoku University, Graduate School of Engineering, Disaster Control Research Centre and also we deeply appreciate to have the permission to use the GIS database summarized by Esri/Zenrin.

REFERENCES

EERI (Earthquake Engineering Research Institute), (2011), "Learning from Earthquakes, The Tohoku, Japan, Tsunami of March 11, 2011": Effects on Structures, EERI Special Earthquake Report

GIA(Geospatial Information Authority of Japan), (2010), "The aerial photo of damaged area of the East Japan Great Earthquake (before and after the occurring disaster)" : Home page of Geospatial Information Authority of Japan

Horie, K., Hayashi, H., Tanaka, S., Hasegawa, K., Maki, N., Okimura, T. (2003), "Construction of the damage function reflecting the degree of damage of the wooden building caused by an earthquake." Technical article No.5, Institute of Regional Safety

Kawasaki, A., Yoshida, S. (2008), "Illustration of ArcGISPart2 GIS (Step-up for practice): published by Kokin Shoin

Koshimura, S., Sugaba, S. (2010), "Reconsideration of the house damage of Tsunami of Hokkaido Southwest Off Earthquake of year 1993. (For the construction of the tsunami damage function)": Technical article No.3, Series 10, 2010, Association for Earthquake Engineering of Japan

Murao, O., Yamazaki, F. (2000), "The building damage function of the Hyogo Prefecture Southern Earthquake based on the results of an autonomy damage investigation.": Structural system article No.527, Architectural Institute of Japan

NILIM(National Institute for Land and Infrastructure Management), Ministry of Land, Infrastructure, Transport and Tourism, Japan) & BRI(Building Research Institute), Incorporated Administrative Agency, Japan, (2011), "Summary of the Field Survey and Research on The 2011 0ff the Pacific coast of Tohoku Earthquake (the Great East Japan Earthquake)", Technical Note of National Institute for Land and Infrastructure Management, No.647, BRI Research Paper, No.150,